WILEY | Hindawi

Research Article

Impact of Geological Factors on Marine Shale Gas Enrichment and Reserve Estimation: A Case Study of Jiaoshiba Area in Fuling Gas Field

Siyu Yu [ID],[1,2] **Xixin Wang** [ID],[1,2] **Shaohua Li,**[1,2] **Yuming Liu** [ID],[3] **Liming Xiao** [ID],[1,2] **Xin Liu** [ID],[1,2] **Wen Zhao** [ID],[4] **and Jiaen Zhang** [ID][5]

[1]*Key Laboratory of Exploration Technologies for Oil and Gas Resources, Yangtze University, Wuhan 430100, China*
[2]*School of Geosciences, Yangtze University, Wuhan 430100, China*
[3]*College of Geosciences, China University of Petroleum, Beijing 102249, China*
[4]*China Petrochemical Press, Beijing 100029, China*
[5]*Daqing Oilfield Co. Ltd. Downhole Service Sub-Company, Daqing 163000, China*

Correspondence should be addressed to Xixin Wang; wangxixin86@hotmail.com

Geological factors are key elements to control shale gas enrichment and influence the accurate estimation of shale gas reserve. However, the impact of the main geological factors, such as porosity, mineralogy, and organic matter, on marine shale gas enrichment and reserve calculation has not yet been fully clarified. Herein, we measured gas adsorption, porosity, mineralogical composition, and total organic carbon content of the marine shale samples from the Jiaoshiba area of Fuling gas field in Sichuan Basin, South China, and investigate the relationships between the geological factors and the adsorbed gas content. The results show that adsorbed gas content is positively correlated with total organic carbon and porosity; the larger specific surface area of samples with more clay minerals essentially contributes to shale gas enrichment. Additionally, the sealing of faults imposes a significant impact on shale gas accumulation. The probability volume method was applied to calculate the shale gas reserve. The reserves of P_{90} (the most pessimistic reserve), P_{50} (the most likely reserve), and P_{10} (the most optimistic reserve) were calculated, respectively, which provides useful information to reduce the risk in shale gas development.

1. Introduction

Shale gas, as a new type of clean energy, has recently influenced the world's energy supply pattern because of the large reserves and wide distribution around the world [1]. The shale gas production of the USA is $6669 \times 10^8 \text{ m}^3$, accounting for 63.4% of the total natural gas production [2, 3]. The recoverable resources of shale gas in China are about $2600 \times 10^{10} \text{ m}^3$, and the resource potential is also huge [4, 5]. The accumulation mechanism of shale gas is complex and has the characteristics of self-generation, self-storage, and self-protection [6, 7]. Thus, the accurate evaluation of the scale and quantity is relatively difficult. According to the different characteristics of shale gas reserves, taking appropriate

resource assessment methods is of great significance for the future exploration and development of shale gas.

Many different geological factors control shale gas enrichment, such as porosity, pore structure, total organic carbon (TOC), clay, and the structural characteristics of strata [8, 9]. The marine shale gas in South China is more complex because of the heterogeneity of shale organic matter content, mineral composition, and other evolutionary conditions [10–12]. At present, the geological factors controlling shale gas enrichment in southern China are still unclear [13, 14]. The research about the relationship between shale gas supply, gas storage, gas preservation, structural style, and spatial-temporal matching of reservoir formation is urgently needed [15–18].
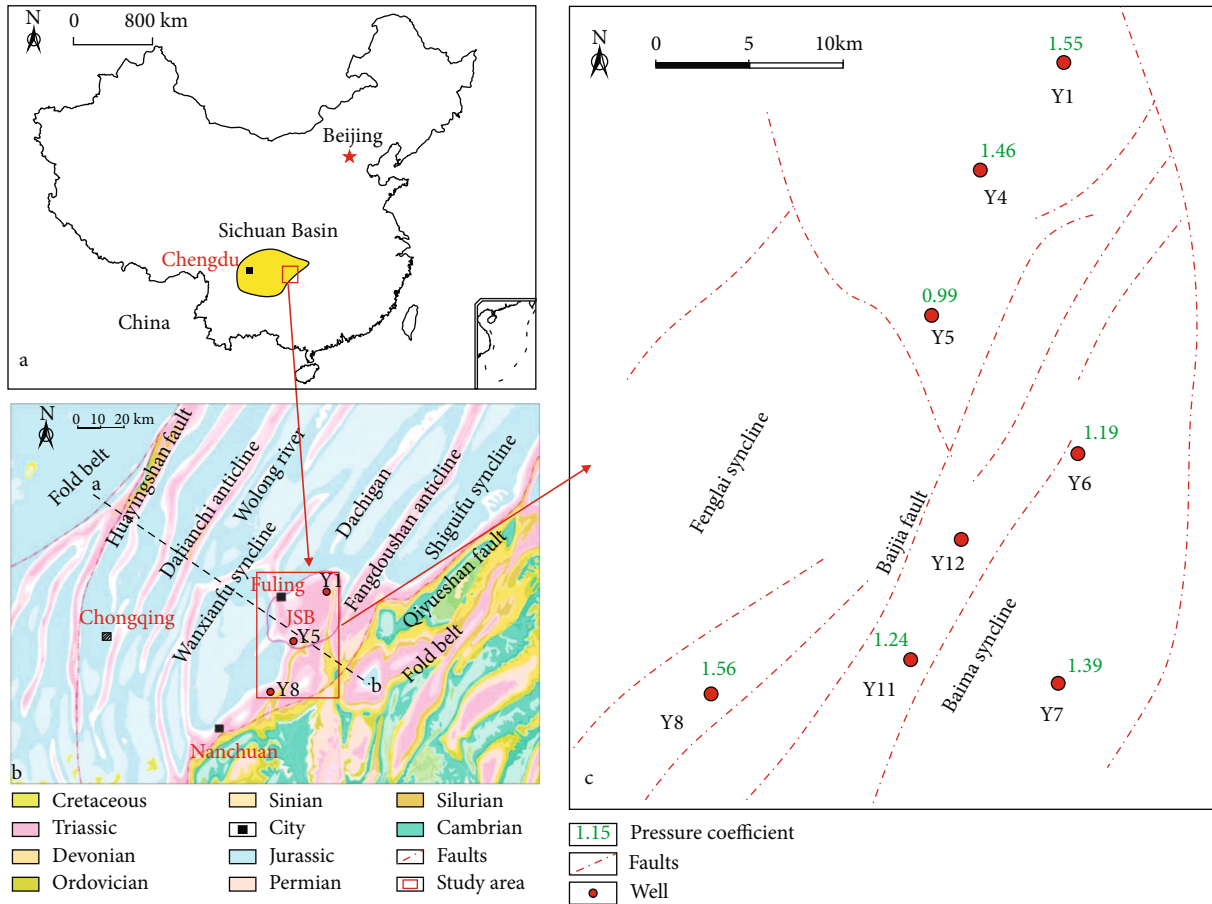
Figure 1: (a) Sichuan Basin; (b) the regional location of Fuling shale gas field; (c) Faults distribution in the JSB area (modified after [30]).

The volume method is generally used for resource calculation [19, 20]. However, due to the complicated accumulation mechanism of natural gas in unconventional reservoirs, shale gas reservoirs usually do not have a clear physical boundary, and the related parameters in the calculation of reserves are difficult to determine. Therefore, the probabilistic volume method is currently an ideal method for shale gas reserve assessment [21–23]. Shale gas resource evaluation method and evaluation parameter assignment have been explored [24]. The principle and method of calculating shale gas resources by volume method are described in detail [25]. Zhang et al. applied the probabilistic volume method to evaluate shale gas resources based on the current situation of shale gas exploration and development in China [26]. According to the principle of the probabilistic volume method [27, 28], the parameters for reserve calculation were selected, assigned, analyzed, and characterized, which not only reflects the uncertainty in the calculation but also ensures accuracy within a certain risk range.

In this study, the relationships between various geological factors and adsorbed gas content were established, and the main geological factors controlling shale gas enrichment were investigated. In the process of reserves calculation, only 18 tests were required to calculate the probability distribution of shale gas reserves using the orthogonal test design method, which greatly improved the efficiency of the calculation and
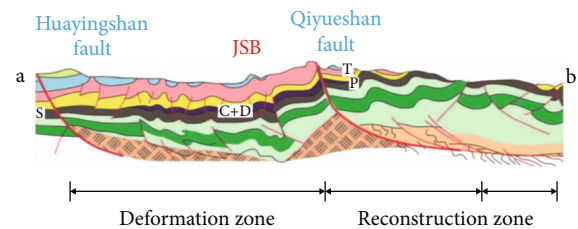

Figure 2: The profile of the structural deformation area of Sichuan Basin (modified after [30]).

provided a basis for the formulation of development plans and reduced development risks.

2. Geological Setting

The Fuling Shale Gas Field is located in the east of the Sichuan Basin (Figure 1(a)), west of the Qiyueshan Fault, and Chuandong barrier-type fold-thrust belt. The main shale gas reservoirs are found in the Jiaoshiba (JSB) area, which is a NE-trending anticline with diamond-shaped controlled by two groups, NE-trending faults and NS-trending faults (Figure 1(b)). The top of the JSB area has a gentle slope without faults, while the two wings of the structure show a steep dip angle and well-developed faults. The partition
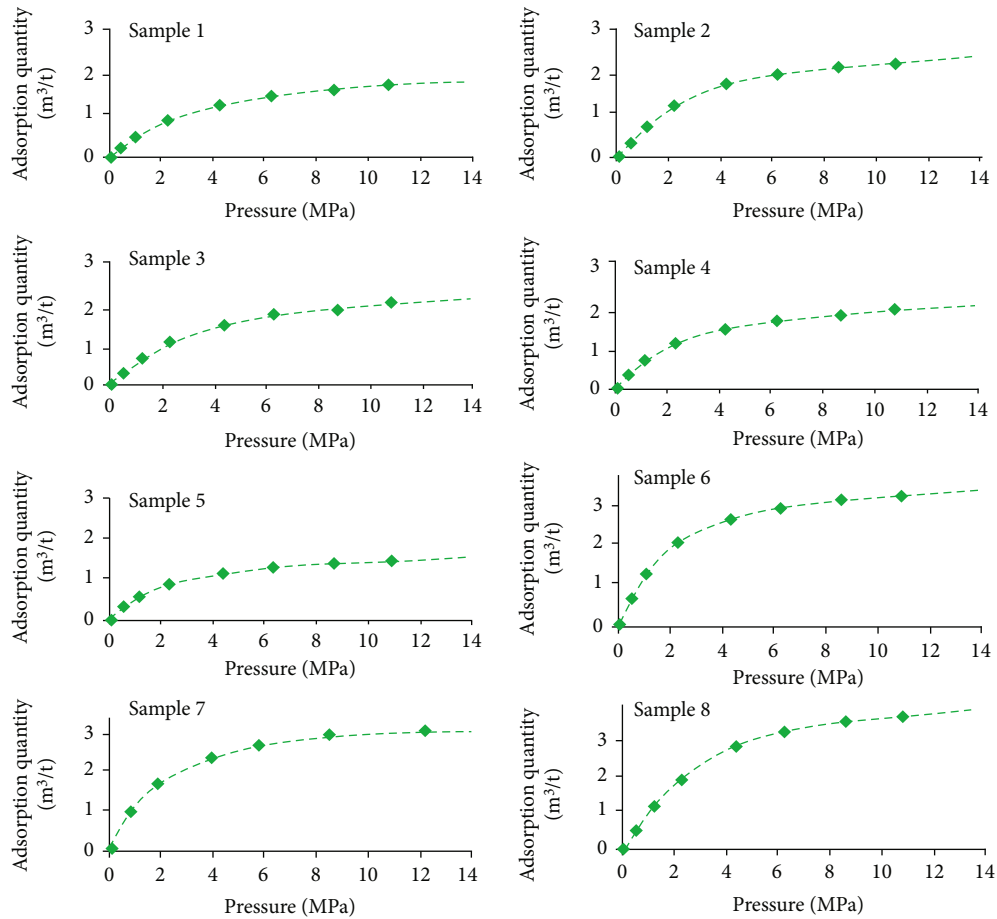
FIGURE 3: Adsorption isotherms of eight shale samples from Wufeng-Longmaxi Formation, JSB area in Fuling gas field.

deformation zone inside the basin is developed in the west of the Qiyueshan fault zone. The Qiyueshan fault zone has good vertical and horizontal continuity. It is characterized by the development of low-microamplitude fold structural styles with little tectonic erosion. The section position of Figure 2 is shown in Figure 1(b). Figure 2 shows that the JSB area, located in such a tectonic background, has well-developed Mesozoic and Paleozoic stratigraphy, which provides good conditions for oil and gas preservation.

The drilled wells showed that the sedimentary environment of Wufeng-Longmaxi Shale varies upward gradually from a deep-water continental shelf to a shallow-water continental shelf environment. The continuous thickness of the shale with a TOC content of more than 2% is over 30 m in Wufeng-Longmaxi Formations. Eight exploration wells from the Y1 well to the Y8 well and nearly 200 development wells were conducted in the main body of the JSB area. The organic-rich shale in the JSB area is well distributed on the plane. The thickness of the high-quality shale reservoir varies from 38 m to 48 m. The lithology of the top gas formation in the JSB area is mainly composed of gray-black clay silty shale, gray-black silty clay mixed shale, and silty clay rock with bands or agglomerate pyrite [29]. The high-quality shale reservoir at the bottom of Wufeng-Longmaxi Formations has the characteristics of high clay content, low siltstone content, high carbon content, and well-developed fractures.
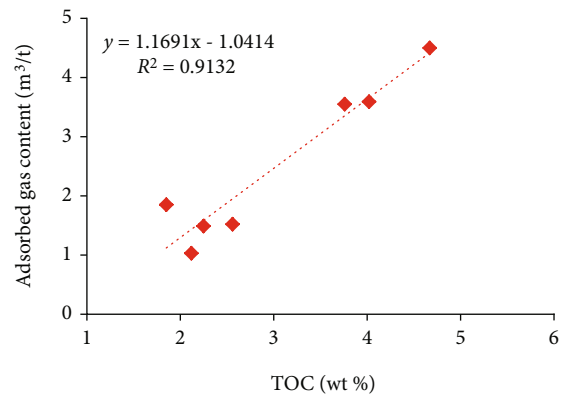
FIGURE 4: Relationship between TOC and adsorbed gas content of samples from Wufeng-Longmaxi Formation, JSB area in Fuling gas field.

3. Samples and Methods

3.1. Samples. Eight shale samples were collected from the lower part of Wufeng-Longmaxi Formations. The samples were divided into several parts for different experiments. First, the density of shale samples that were cut into cylinders was measured using the volumetric method. Porosity measurement was performed by ULTRA PORO300 Porosity,

FIGURE 5: The relationship between (a) carbonate content, (b) carbonate minerals content, and adsorbed gas content.

following the standard GB/T 29172-2012 of China (GB/T 29172-2012). The pure calcium carbonate (0.2 g) and the shale sample powder (0.2 g) were mixed with enough dilute hydrochloric acid, respectively. The carbonate content of shale samples can be obtained by comparing the pressure of carbon dioxide.
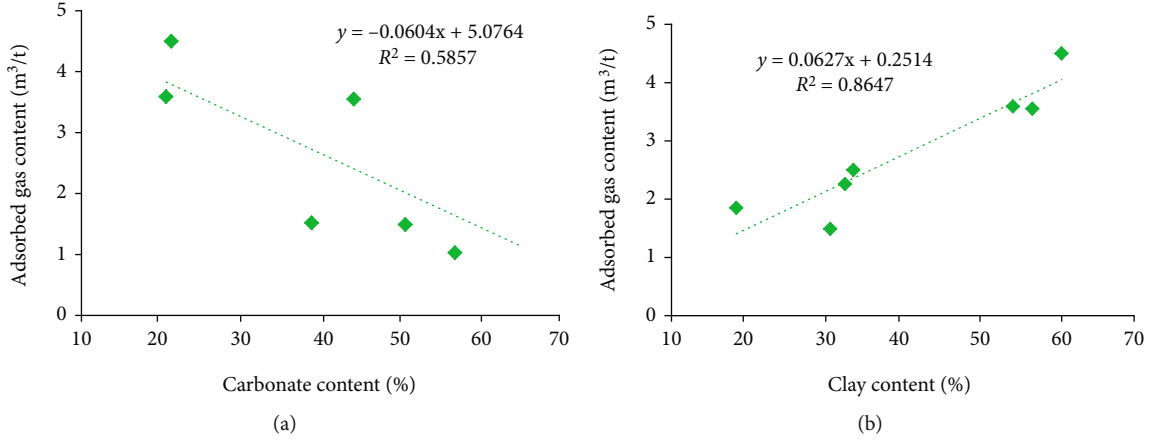
3.2. Experiment and Calculation Methods. The samples, which were crushed into ~150 mesh using SPEX 8000 M Mixer/Mill, were mixed with ethanol and then laid on glass slides. Dmax-2500 X-ray diffractometer (XRD) was used to test the clay content. Before the TOC test, the inorganic carbon in the samples was removed using hydrochloric acid (4%-4.13%). The Cornerstone™ carbon-sulfur analyzer that combusts a 130 mg sample of powdered shale samples was used to test the TOC content at 704.4°C [3, 31].

Isothermal adsorption experiments were conducted by using GAI-100 high-accuracy isotherm instrument and AJP-100 volume calibrator. The maximum working pressure of GAI-100 is 10000 Psi (69 MPa), and the accuracy of the pressure sensor is 0.05%. The eight samples were crushed into 50-80 mesh size, and the adsorbed moisture and capillary water in the samples were removed at around 120°C for approximately 24 h. The isotherms were obtained under pressure ranging from 0.01 to 14 MPa at 177°C. The accuracy of the temperature sensor is 0.1°C. The maximum adsorption volume can be calculated by the software automatically using Langmuir theory [32, 33].

According to the basic principle of the probabilistic volume method, the amount of shale gas resources is the probability product of shale mass and natural gas (gas content) contained in mud shale per unit mass. The calculation formula is as follows:

$$Q_t = 0.01 \times S \cdot H \cdot \rho \cdot q. \tag{1}$$

Q_t is the amount of shale gas resources ($10^8 m^3$); S is the area of gas shale (km^2); H is the effective thickness of shale (m); ρ is the shale density (t/m^3); q is the gas content (m^3/t).

The shale gas content is a key parameter in the calculation and evaluation of shale gas resources. And it is a param-

eter with a large range of numerical values and is difficult to obtain accurately. Therefore, shale gas content can be obtained by using the decomposition method. The mode of occurrence of natural gas could be free, adsorbed, or dissolved, which can be calculated by different methods, as follows:

$$Q_t = q_a + q_f + q_d. \tag{2}$$

q_a is the adsorption gas content (m^3/t), q_f is the free gas content (m^3/t), and q_d is the dissolved gas content (m^3/t).

At present, the main method to obtain adsorption gas content is the isothermal adsorption experiment. The samples were placed in the environment of approximate underground temperature, and the maximum adsorbed gas was measured under different pressure conditions as follows:

$$Q_a = 0.01 \times S \cdot H \cdot \rho \cdot q_a, \tag{3}$$

$$q_a = V_L \cdot P/(P_L + P). \tag{4}$$

q_a is the adsorption gas content (m^3/t), V_L is the Langmuir volume (m^3), P_L is the Langmuir pressure (MPa), and P is the stratum pressure (MPa).

The free gas content (q_f) can be obtained by porosity (including pore and fracture volume) and gas saturation [34], as follows:

$$Q_f = 0.01 \times S \cdot H \cdot \rho \cdot q_f, \tag{5}$$

$$q_f = \phi_g \cdot S_g/B_g. \tag{6}$$

Φ_g is the porosity (%), S_g is the gas saturation (%), and B_g is the volume factor, which is used to convert the volume of underground natural gas into the volume under standard conditions.

Natural gas in shale can be dissolved in the formation water, kerogen, asphaltene, or crude oil to varying degrees. Because the natural gas content dissolved in kerogen and
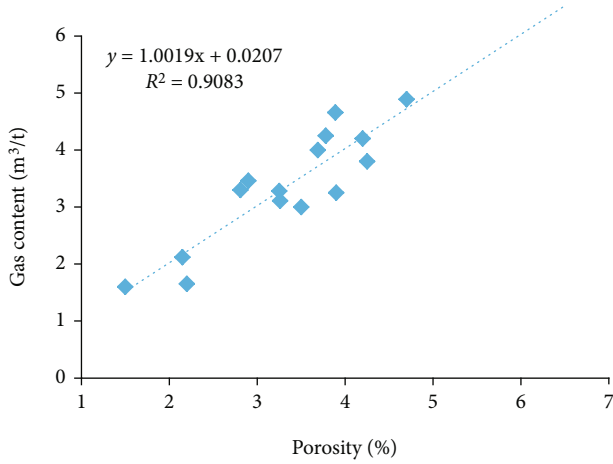
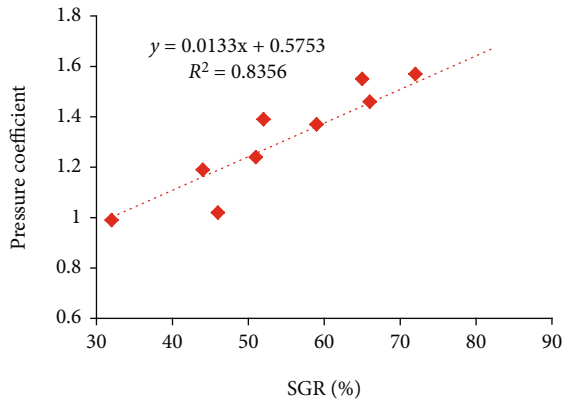Figure 6: Relationship between porosity and adsorbed gas content.

Figure 7: The relationship between SGR index and pressure coefficient.

Table 1: Five factors and three levels orthogonal table.

Shale density	TOC	Porosity	Gas saturation	Shale gas volume coefficient
-1	-1	-1	-1	-1
0	0	0	0	0
1	1	1	1	1

Table 2: The calculation results of shale gas reserves of 18 tests.

No.	ρ	TOC	φ	S_g	B_{gi}	G_a ($10^8 m^3$)	G_f ($10^8 m^3$)	G_t ($10^8 m^3$)
1	1	1	1	1	1	55.37	81.74	137.11
2	1	0	0	0	0	54.63	71.52	126.15
3	1	-1	-1	-1	-1	54.39	61.30	115.69
4	0	1	1	0	0	54.83	75.10	130.93
5	0	0	0	-1	-1	54.09	64.53	118.62
6	0	-1	-1	1	1	53.85	73.95	127.80
7	-1	1	0	1	-1	54.28	86.04	140.32
8	-1	0	-1	0	1	53.55	64.71	118.26
9	-1	-1	1	-1	0	53.30	64.37	117.67
10	1	1	-1	-1	0	55.37	58.24	113.61
11	1	0	1	1	-1	54.63	90.34	144.97
12	1	-1	0	0	1	54.39	68.12	122.51
13	0	1	0	-1	1	54.83	58.39	113.22
14	0	0	-1	1	0	54.09	77.65	131.74
15	0	-1	1	0	-1	53.85	79.05	132.90
16	-1	1	-1	0	-1	54.28	71.52	125.80
17	-1	0	1	-1	1	53.55	61.30	114.85
18	-1	-1	0	1	0	53.30	81.74	135.04

asphaltenes is tiny, and the formation water is not the main fluid of shale, the dissolved gas content can be ignored in gas content analysis.

4. Results and Discussion

4.1. Relationship between the TOC and Adsorption Gas Content. The isotherms of the samples were shown in Figure 3, indicating that the lower part of the shale in Wufeng-Longmaxi Formations had good adsorption performance, and the content of adsorbed gas in the shales has a positive correlation with pressure. Wufeng-Longmaxi Shale in the study area is mainly developed in shallow water and deep-water continental shelf sedimentary environments. The continuous thickness of the shale with TOC content larger than 2% is over 30 m. The organic matter in the shale not only controls the pore structure but also significantly controls the adsorbed gas content in the shale. Figure 4 shows that the adsorbed gas content in shale samples increases with the content of TOC. This is because the presence of organic carbon generates more organic pores and larger specific surface area in the samples, which can increase the adsorbed gas content [35–37]. The relationships have been suggested in previous studies on shales from some North American basins [38, 39].

4.2. Relationship between Clay, Carbonate Content, and Adsorbed Gas Content. Figure 5(a) shows the relationship between the carbonate content and the adsorbed gas content in the shale samples. It can be seen that as the content of carbonate increases, the content of adsorbed gas in the sample decreases; this is because the presence of carbonate minerals occupies the pore space, which reduces the specific surface area of the shale samples and content of adsorbed gas. However, as shown in Figure 5(b), as the clay mineral content increases, the adsorbed gas content in the samples gradually increases. This is because the presence of clay minerals increases the pores and their related specific surface area of the samples [14, 31, 40, 41], which can absorb more natural gas in the shale.

4.3. Relationship between Porosity and Adsorbed Gas Content. The porosity of Wufeng-Longmaxi Shale gas reservoirs in the JSB area of the Fuling gas field is between 1.45% and 6.38%, with an average of about 3.65%. The overall porosity is relatively high, which provides good conditions for natural gas storage. Figure 6 shows a positive correlation between porosity and gas content in the samples; that means
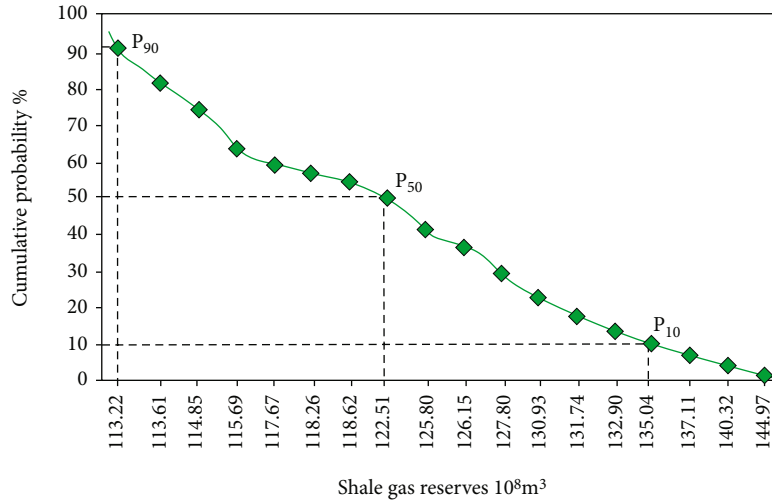
FIGURE 8: Cumulative probability distribution of shale gas reserves in JSB area.

that porosity has a significant control effect on the gas content of the shale. The porosity of gas reservoirs in the lower part of Wufeng-Longmaxi Formations is significantly higher than that of the upper part. The TOC in the lower part is significantly higher than that of the upper gas layer. This could be the main reason for the significant difference in the total amount of adsorbed gas and free gas between the lower part and upper part of Wufeng-Longmaxi Formations.

4.4. Relationship between Regional Tectonic Deformation and Shale Gas Content.

The intense tectonic movement promoted many large faults, making the shale gas preservation conditions in the Fuling area vary greatly. The strength of structural deformation in the Fuling area is gradually weakened from east to west. The scale of the faults in the Baima syncline belt is very large. As a result, the pressure coefficient in the east is about 1.2, and the pressure coefficient in some areas with few faults exceeds 1.3, reflecting the poor preservation conditions in the eastern tectonic belt. The pressure coefficient of Fenglai syncline and JSB anticline is larger than 1.2, and some areas (Y8 and Y10 well area) exceed 1.5, reflecting that the overall gas preservation of the West Belt is in good condition, as shown in Figure 1(c).

Also, fault sealing has a significant control effect on the shale gas content [3]. In this study, the shale gouge ratio (SGR) index is used to evaluate the fault sealability quantitatively [42–44]. SGR index refers to the proportion of mud that is squeezed into the fault zone due to various mechanisms or dynamics (Formula (7)). A larger SGR indicates the better lateral sealing of faults. It can be seen from the relationship between the SGR index and the pressure coefficient of a single well, the better the fault sealing, the greater the pressure coefficient, indicating more gas content in the shale reservoirs (Figure 7).

$$\text{SGR} = \frac{\sum_{i=1}^{n}(H_i \times S_i)}{H} \times 100\%. \tag{7}$$

n is the number of broken stratum, H_i is the thickness of

broken stratum, S_i is the clay content of broken stratum, and H is the total thickness of broken strata.

4.5. Reserve Calculation

4.5.1. Parameter Optimization and Assignment.
Based on the above analysis, TOC, the shale gas density, porosity, gas saturation, and original natural gas volume coefficient are selected as the main parameters for calculating shale gas reserves in the study area. To calculate shale gas reserves based on three-dimensional geological models, the construction model, the shale density model, the TOC model, the porosity model, and the gas saturation model were established by using the Sequential Gaussian method.

The value of shale density was analyzed statistically from samples. The minimum value was 2.4 g/cm³, the maximum value was 2.8 g/cm³, and the average value was 2.6 g/cm³. The density is mainly distributed in 2.55-2.65 g/cm³. The -1% model, the benchmark model, and the +1% model are regarded as the pessimistic value, the possible value, and the optimistic value, respectively. TOC, porosity, and the original natural gas volume coefficient are also taken from three equal percentage levels. The -5% model, the benchmark model, and the +5% model are regarded as the pessimistic value, the possible value, and the optimistic value. The -10% model, the benchmark model, and the +10% model of the gas saturation are regarded as the pessimistic value, the possible value, and the optimistic value.

4.5.2. Calculation of Shale Reserves Based on Probability Volume Method.
Three levels of pessimism (-1), possibility (0), and optimism (1) were selected for each type of uncertain parameters affecting shale gas reserves. A factor level table was established for the calculation, as shown in Table 1.

If the five factors in the three levels are fully designed, we must establish 243 models and calculate the reserves. In this study, the experimental design method was used to analyze the uncertain parameters that affect the reserve. Only 18 tests were required to calculate the probability distribution of

shale gas reserves, which greatly improved the calculation efficiency. Also, the geological factors that affect the calculation of reserves can be quantitatively evaluated through the analysis of variance. The adsorbed gas (G_a) and the free gas (G_f) are calculated, respectively, and then the total reserves (G_t) are calculated, as shown in Table 2.

The geological process and its products can be regarded as random events; that means various geological observations have random variables. Thus, the method of probability statistics can be used to study the regularity of geological variable changes. The method of orthogonal test design is used to evaluate the uncertainty of geological variables, and the cumulative probability distribution curve of shale gas reserves was obtained (Figure 8). The reserves of P_{90}, P_{50}, and P_{10} were chosen by using the method of queuing probabilistic reserves [45]. The reserves of P_{90}, P_{50}, and P_{10} correspond to the most pessimistic reserve, the most likely, and the most optimistic reserve, respectively. To reduce the risk in shale gas development, the three possible values of shale gas reserves should be fully considered.

5. Conclusion

In this paper, the adsorbed gas content, porosity, mineralogical composition, and total organic carbon content of shale samples from the Jiaoshiba area, Sichuan Basin were investigated using a series of experiments. The following conclusions were obtained:

(1) The main factors controlling the shale gas enrichment of the Fuling gas field are TOC, carbonate content, clay minerals, and porosity. Shales with higher TOC, clay, and porosity have more adsorption gas

(2) Fault sealing has a significant control effect on the enrichment of shale gas. The better the sealing of faults, the greater the pressure coefficient of strata, indicating more shale gas accumulated in the formations

(3) The reserves of P_{90}, P_{50}, and P_{10} correspond to the most pessimistic reserve, the most likely, and the most optimistic reserve, respectively. To reduce the risk in shale gas development, the three possible values of shale gas reserves should be fully considered. The corresponding geological model can be selected for shale gas numerical simulation to evaluate the impact of geological uncertainty on development quantitatively and reduce the risk in shale gas development

Data Availability

All the data can be obtained from the corresponding author.

Conflicts of Interest

The authors declare that they have no conflicts of interest.

References

[1] J. Zhijun, C. Xunyu, L. Jinlian, Z. Yu, and C. Zhe, "The recent exploration progress and resource development strategy of China Petroleum and Chemical Corporation," *China Petroleum Exploration*, vol. 23, pp. 14–25, 2018.

[2] Z. Jiang, Y. Song, X. Tang et al., "Controlling factors of marine shale gas differential enrichment in southern China," *Petroleum Exploration and Development*, vol. 47, pp. 661–673, 2000.

[3] X. Wang, J. Hou, S. Li et al., "Insight into the nanoscale pore structure of organic-rich shales in the Bakken Formation, USA," *Journal of Petroleum Science and Engineering.*, vol. 191, article 107182, 2020.

[4] S. Jiang, X. Ta, and O. Steve, "Enrichment factors and current misunderstanding of shale oil and gas, case study of shales in U.S., Argentina and China," *Earth Science*, vol. 42, pp. 1083–1091, 2017.

[5] G. Zhai, Y. Wang, S. Bao et al., "Major factors controlling the accumulation and high productivity of marine shale gas and prospect forecast in the southern China," *Earth Science*, vol. 42, pp. 1057–1068, 2017.

[6] C. Zou, Q. Zhao, D. Dong et al., "Geological characteristics, main challenges and future prospect of shale gas," *Journal of Natural Gas Geoscience*, vol. 2, no. 5-6, pp. 273–288, 2017.

[7] C. Sondergeld, K. Newsham, J. Comisky, M. Rice, and C. Rai, "Petrophysical considerations in evaluating and producing shale gas resources," in *SPE unconventional gas conference*, p. 2010, Pittsburgh, Pennsylvania, USA, February 2010.

[8] G. L. Sheng, Y. L. Su, and W. D. Wang, "A new fractal approach for describing induced-fracture porosity/permeability/ compressibility in stimulated unconventional reservoirs," *Journal of Petroleum Science and Engineering*, vol. 179, pp. 855–866, 2019.

[9] R. Wang, S. Sang, J. Jin et al., "Characteristics and significance of heterogeneity of sea-land transitional facies shale gas reservoir in North Guizhou, China," *Geosciences Journal*, vol. 23, 2019.

[10] X. Wang, L. Zhang, and G. Chao, "The heterogeneity of lacustrine shale gas reservoir in Yanchang Formation, Xiasiwan area, Ordos Basin," *Acta Geologica Sinica English Edition*, vol. 89, no. s1, pp. 99–101, 2015.

[11] Y. Guo and D. Zhao, "Analysis of micro-scale heterogeneity characteristics in marine shale gas reservoir," *Journal of China University of Mining and Technology*, vol. 44, pp. 300–307, 2015.

[12] K. Wawrzyniak-Guz, J. A. Jarzyna, M. Zych, M. Bała, P. I. Krakowska, and E. Puskarczyk, "Analysis of the heterogeneity of the Polish shale gas formations by factor analysis on the basis of well logs," in *78th EAGE Conference and Exhibition 2016*, Vienna, Austria, 2016.

[13] X. LI, S. CHEN, X. WANG, Y. ZHU, M. CHANG, and C. UWAMAHORO, "Pore structure heterogeneity of the

Xiamaling Formation shale gas reservoir in the Yanshan area of China: evaluation of geological controlling factors," *Acta Geologica Sinica - English Edition*, vol. 93, no. 3, pp. 588–603, 2019.

[14] X. X. Wang, J. G. Hou, S. H. Song et al., "Combining pressure-controlled porosimetry and rate-controlled porosimetry to investigate the fractal characteristics of full-range pores in tight oil reservoirs," *Journal of Petroleum Science and Engineering*, vol. 171, pp. 353–361, 2018.

[15] T. Zhang, H. W. Yin, G. U. Dong et al., "Structural deformation characteristics and shale gas preservation of Lower Yangtze region," *Journal of the China Coal Society*, vol. 38, pp. 883–889, 2013.

[16] B. Kulga and T. Ertekin, "Numerical representation of multicomponent gas flow in stimulated shale reservoirs," *Journal of Natural Gas Science and Engineering*, vol. 56, pp. 579–592, 2018.

[17] J. Sun and B. Luo, "Structural deformation and its influences on gas storage in Fuling shale gas play, the Sichuan Basin," *Oil & gas geology*, vol. 37, pp. 809–818, 2016.

[18] H. Nie, Z. He, R. Wang et al., "Temperature and origin of fluid inclusions in shale veins of Wufeng–Longmaxi Formations, Sichuan Basin, south China, implications for shale gas preservation and enrichment," *Journal of Petroleum Science and Engineering*, vol. 193, article 107329, 2020.

[19] Y. Ran, M. Lannerstad, M. Herrero, C. E. van Middelaar, and I. J. M. de Boer, "Assessing water resource use in livestock production: a review of methods," *Livestock Science*, vol. 187, pp. 68–79, 2016.

[20] H. B. Pratama and M. C. Supijo, "Experimental design and response surface method in geothermal energy: a comprehensive study in probabilistic resource assessment," *Geothermics*, vol. 87, article 101869, 2020.

[21] W. Ren and H. C. Lau, "Analytical modeling and probabilistic evaluation of gas production from a hydraulically fractured shale reservoir using a quad-linear flow model," *Journal of Petroleum Science and Engineering*, vol. 184, p. 106516, 2020.

[22] F. T. Murat and S. Caglar, "A new fully probabilistic methodology and a software for assessing uncertainties and managing risks in shale gas projects at any maturity stage," *Journal of Petroleum Science and Engineering*, vol. 168, pp. 107–118, 2018.

[23] L. Xue, Y. Liu, T. Nan, Q. Liu, and X. Jiang, "An efficient automatic history matching method through the probabilistic collocation based particle filter for shale gas reservoir," *Journal of Petroleum Science and Engineering*, vol. 190, p. 107086, 2020.

[24] Q. Xiaosong, H. Mingyi, H. Zhonggui, Y. Ying, and C. Quansheng, "Evaluation methods and parameter assignments of shale gas resources: a case study of the Wufeng-Longmaxi Formation in the Middle Yangtze region," *Geology in China*, vol. 41, pp. 2091–2098, 2014.

[25] W. Z. Xu, *Principle and Method of Shale Gas Resources Calculation by Volume Method-Case of ES2 Formation in LF Fault Depression*, p. 7, 2019.

[26] J. Zhang, L. Lin, Y. Li et al., "Methods and techniques for shale gas resource evaluation: probabilistic volume method," *Earch Science Frontiers*, vol. 19, pp. 184–192, 2012.

[27] A. A. Kaufman, "Methods in geochemistry and geophysics principles of the gravitational method volume 41 chapter 3 principles of measurements of the gravitational field," *Methods in Geochemistry & Geophysics*, vol. 41, pp. 161–215, 2007.

[28] G. S. Kruglik, "Derivation of the equations of probabilistic method with account taken of the identity principle," *Vesci Akad. Navuk BSSR Ser. Fiz.-Tèhn. Navuk*, vol. 3, pp. 45–50, 1963.

[29] Z. Shu, D. Fang, A. Zheng et al., "Geological characteristics and development potential of upper shale gas reservoirs of the 1st member of Longmaxi Formation in Jiaoshiba area, Sichuan Basin," *Natural Gas Geoscience*, vol. 31, pp. 393–402, 2020.

[30] X. S. Guo, "Controlling factors on shale gas accumulations of Wufeng-Longmaxi Formations in Pingqiao shale gas field in Fuling area, Sichuan Basin," *Natural Gas Geoscience*, vol. 30, pp. 1–10, 2019.

[31] K. Liu, M. Ostadhassan, and X. M. Xu, "A comparison study of the unloading behavior in shale samples in nanoindentation experiments using different models," *Journal of Petroleum Science and Engineering*, vol. 186, p. 106715, 2020.

[32] D. Avnir and M. Jaroniec, "An isotherm equation for adsorption on fractal surfaces of heterogeneous porous materials," *Langmuir*, vol. 5, no. 6, pp. 1431–1433, 1989.

[33] P. I. Ravikovitch, A. Vishnyakov, R. Russo, and A. V. Neimark, "Unified approach to pore size characterization of microporous carbonaceous materials from N2, Ar, and CO2 adsorption isotherms," *Langmuir*, vol. 16, no. 5, pp. 2311–2320, 2000.

[34] J. C. Zhang, L. M. Lin, Y. X. Li et al., "The method of shale gas assessment: probability volume method," *Earth Science Frontiers*, vol. 19, pp. 184–191, 2012.

[35] X. Shao, X. Pang, Q. Li et al., "Pore structure and fractal characteristics of organic-rich shales: a case study of the lower Silurian Longmaxi shales in the Sichuan Basin, SW China," *Marine and Petroleum Geology*, vol. 80, pp. 192–202, 2017.

[36] G. L. Sheng, H. Zhao, Y. L. Su et al., "An analytical model to couple gas storage and transport capacity in organic matter with noncircular pores," *Fuel*, vol. 268, p. 117288, 2020.

[37] C. R. Clarkson, N. Solano, R. M. Bustin et al., "Pore structure characterization of North American shale gas reservoirs using USANS/SANS, gas adsorption, and mercury intrusion," *Fuel*, vol. 103, pp. 606–616, 2013.

[38] D. J. K. Ross and R. M. Bustin, "The importance of shale composition and pore structure upon gas storage potential of shale gas reservoirs," *Marine and Petroleum Geology*, vol. 26, no. 6, pp. 916–927, 2009.

[39] G. R. Chalmers, R. M. Bustin, and I. M. Power, "Characterization of gas shale pore systems by porosimetry, pycnometry, surface area, and field emission scanning electron microscopy/transmission electron microscopy image analyses: examples from the Barnett, Woodford, Haynesville, Marcellus, and Doig unit," *AAPG Bulletin*, vol. 96, no. 6, pp. 1099–1119, 2012.

[40] Y. Han, D. Kwak, S. Choi, C. Shin, Y. Lee, and H. Kim, "Pore structure characterization of shale using gas physisorption: effect of chemical compositions," *Minerals*, vol. 7, no. 5, p. 66, 2017.

[41] X. X. Wang, Y. M. Liu, J. G. Hou et al., "The relationship between synsedimentary fault activity and reservoir quality - a case study of the Ek1 formation in the Wang Guantun area, China," *Interpretation*, vol. 8, no. 3, pp. sm15–sm24, 2020.

[42] T. Fristad, A. Groth, G. Yielding, and B. Freeman, "Quantitative fault seal prediction: a case study from Oseberg Syd," *Norwegian Petroleum Society Special Publications*, vol. 7, pp. 107–124, 1997.

[43] D. Harris, G. Yielding, P. Levine, G. Maxwell, P. T. Rose, and P. Nell, "Using Shale Gouge Ratio (SGR) to model faults as transmissibility barriers in reservoirs: an example from the Strathspey Field, North Sea," *Petroleum Geoscience*, vol. 8, no. 2, pp. 167–176, 2002.

[44] P. Bretan, G. Yielding, and H. Jones, "Using calibrated shale gouge ratio to estimate hydrocarbon column heights," *AAPG Bulletin*, vol. 87, no. 3, pp. 397–413, 2003.

[45] X. Bao, S. H. Li, C. Zhang, B. Qiao, J. Li, and H. M. Di, "Application of probability volume method based on experimental design to calculation of shale gas reserves," *Fault block oil gas field*, vol. 24, pp. 678–681, 2017.